Cell. Mol. Life Sci. 63 (2006) 2364–2376
1420-682X/06/202364-13
DOI 10.1007/s00018-006-6166-8

Cellular and Molecular Life Sciences

Research Article

Melanoma cells exhibit strong intracellular TASK-3-specific immunopositivity in both tissue sections and cell culture

K. Pocsai [a], L. Kosztka [a], G. Bakondi [a], M. Gönczi [a], J. Fodor [a], B. Dienes [a], P. Szentesi [a], I. Kovács [b], R. Feniger-Barish [c], E. Kopf [c], D. Zharhary [c], G. Szűcs [a], L. Csernoch [a, d] and Z. Rusznák [a, *]

[a] Department of Physiology, RCMM, Medical and Health Science Centre, University of Debrecen, P.O. Box 22, 4012 Debrecen (Hungary), Fax: +36 52 432 289, e-mail: rz@phys.dote.hu
[b] Department of Pathology, HBM Kenézy Gyula County Infirmary, Bartók Béla u. 2–26, 4043 Debrecen (Hungary)
[c] Sigma-Aldrich Israel, Rehovot (Israel)
[d] Cell Physiology Research Group of the Hungarian Academy of Sciences, University of Debrecen, Debrecen (Hungary)

Received 12 April 2006; received after revision 10 July 2006; accepted 8 August 2006
Online First 28 September 2006

Amplification of the kcnk9 gene and overexpression of the encoded channel protein (TASK-3) seems to be involved in carcinogenesis. In the present work, TASK-3 expression of melanoma cells has been studied. For the investigation of TASK-3-specific immunolabelling, a monoclonal antibody has been developed and applied along with two, commercially available polyclonal antibodies targeting different epitopes of the channel protein. Both primary and metastatic melanoma cells proved to be TASK-3 positive, showing prominent intracellular TASK-3-specific labelling; mostly concentrating around or in the proximity of the nuclei. The immunoreaction was associated with the nuclear envelope, and with the processes of the cells and it was also present in the cell surface membrane. Specificity of the immunolabelling was confirmed by Western blot and transfection experiments. As TASK-3 immunopositivity of benign melanocytes could also be demonstrated, the presence or absence of TASK-3 channels cannot differentiate between malignant and non-malignant melanocytic tumours.

Keywords. TASK-3 channel, melanoma, melanocyte, immunocytochemistry, immunohistochemistry, monoclonal antibody, transfection, Western blot.

Introduction

TASK-3 channels belong to the recently discovered two-pore-domain (2P) K^+ channel superfamily [1]. In contrast to the other two known K^+ channel superfamilies [voltage-gated or depolarisation-activated K^+ (Kv) channels and inwardly rectifying K^+ (Kir) channels], whose representatives form tetramers; in the 2P channels two subunits associate with each other, thus the functional channels are dimers. However, as each subunit of the 2P channels contains four transmembrane domains and two pore-forming loops (the latter situated in a 'tandem' arrangement), the K^+ permeable pore of the 2P channels is produced by the interaction of four individual pore-forming regions, similarly to the more 'conventional' K^+ channels. The individual representatives of the 2P channels belong to a number of smaller classes within the 2P superfamily, one of which is formed by the TWIK-related acid-sensitive K^+ channels (TASK channels; [2–12]).

Three channels belonging to the TASK family are known at present, termed TASK-1, TASK-3, and TASK-5. (Although TASK-2 and TASK-4 channels have also been cloned, analysis of their amino acid sequence clearly indicated that they are not as close relatives of the other

* Corresponding author.

TASK channels as thought initially, thus they are now regarded as members of the TALK channel family.) The close relationship between TASK-1, TASK-3, and TASK-5 channels is convincingly substantiated by their sequence homology: the sequence identity between hTASK-1 and hTASK-3 channels is about 62% [3], whereas hTASK-5 shows 58% and 56% identity with hTASK-1 and hTASK-3, respectively [13]. In contrast, sequence identity between the TASK channels and the rest of the 2P channels is as low as 31–35% [3].

A common functional property of the TASK channels is their closure on extracellular acidification; the pK for TASK-3 is about 6.8 [3, 9, 11, 14]. Initially, TASK channels were thought to be important for setting the high resting K^+ conductance of the cells, determining therefore their resting membrane potential, input resistance and excitability only. More recent experiments, however, clearly indicated that TASK-3 channels belong to a most intriguing group of K^+ channels having the seemingly paradoxical ability to either induce [15] or prevent apoptotic cell death [16] and promote cell proliferation [17, 18]. The potential pathological significance of the TASK-3 channels emerged when amplification of the TASK-3 coding gene (kcnk9) was reported in 10% of the malignant breast tumours investigated, along with a 5–100-fold overexpression of the channel protein in 44% of the tumour specimens [17]. Although kcnk9 is situated at the chromosomal region 8q24.3, in the proximity of a well-known oncogene (c-myc), kcnk9 amplification alone was found to be present in a number of cases, suggesting its potential causative role in tumour development.

Experiments conducted on cell lines overexpressing either the wild-type TASK-3 channels or a non-functional mutant (TASK-3^{G95E}), convincingly proved the previous implications concerning the significance of the functional TASK-3 channel proteins in tumorigenesis [18]. Overexpression of the wild-type TASK-3 enhanced tumorigenicity of C8 cells and shortened the time for tumour formation in athymic mice. Moreover, cultured C8 cells became more resistant for hypoxia and serum deprivation. The Ben cell line (lung carcinoma) is known to naturally overexpress TASK-3 channels; transfection of these cells with TASK-3^{G95E} (which proved to be a dominant negative mutation) resulted in a significant reduction of cell proliferation. Based on these experiments, kcnk9 is an established proto-oncogene, whose amplification (along with the overexpression of the encoded protein) may favour tumour formation, most likely via increasing the resistance of cancer cells for hypoxia and serum deprivation – a mechanism which might powerfully increase the survival of cancer cells, especially in the poorly oxygenated areas of solid tumours.

Hitherto no correlation has been found between the TASK-3 expression of malignant tumours and the presence or absence of certain tumour/prognostic markers (oestrogen receptor expression and HER2 overexpression [17]), but it cannot be excluded that such connections might be revealed in the not too distant future, and/or TASK-3 might eventually serve as a histological tumour marker itself. However, to prove or disprove this assumption, large scale immunohistochemical studies are required using TASK-3-specific primary antibodies. Although anti-TASK-3 polyclonal antibodies are currently available commercially and their applicability has already been documented in a number of studies [19–24], the development and evaluation of a TASK-3-specific monoclonal antibody would be important as monoclonal antibodies are regarded far superior to the polyclonal ones.

In the present study three different anti-TASK-3-specific antibodies (two polyclonal and a newly developed monoclonal) were employed to investigate the possible TASK-3-protein expression of melanoma cells; as it was potentially interesting to see whether – similarly to certain breast cancers, colorectal cancers and to the Ben cell line – prominent TASK-3 immunopositivity was also present in these malignantly transformed cells. Moreover, we invesitgated whether only the melanoma cells showed TASK-3 expression or whether the TASK-3 protein was also present in benign melanocytes.

In the present study, immunoreactions were performed on formaldehyde-fixed, paraffin-embedded tissue sections and cultured melanoma cells, and the evaluation of the antibodies was also extended to cell lines transiently or stably transfected with TASK-3. Our results indicate that all three primary antibodies investigated are capable of recognising TASK-3 channels under both immunohistochemical and immunocytochemical conditions. In formaldehyde-fixed sections, the intensity of the labelling could be improved using an appropriate antigen-retrieval (AR) technique. In both preparations, the TASK-3-immunopositivity showed markedly strong intracellular distribution. It was concluded that as both malignant melanoma cells and benign melanocytes demonstrated TASK-3 immunopositivities, TASK-3 labelling is not applicable to differentiating between malignant and benign melanocytic tumours, further confirming the generally accepted view that there is no 'melanoma antibody' (for a review see [25]).

Materials and methods

Development of a monoclonal anti-hTASK-3 antibody. The monoclonal anti-KCNK9 (TASK-3) (clone KCN-75) was raised against a synthetic peptide corresponding to amino acids 360–374 of the C terminus of human KCNK9. For immunization, the peptide was conjugated to KLH using the Maleimide Activated BSA/KLH Conjugation Kit (Sigma-Aldrich, MBK-1). BALB/c mice were immunized and their spleen cells were fused with NS-1 mouse myeloma cells. Hybridoma supernatants were screened

for specific antibodies by ELISA on a BSA conjugate of the above peptide and by Western blotting of cell extracts. One clone termed KCN-75, which secretes IgG2b antibodies (Sigma Immunotype™ kit ISO-2) was selected. The antibody was purified on a protein A column and was supplied by Sigma-Aldrich (Sigma, K0514).

Immunohistochemistry. The immunohistochemical methods were similar to those reported earlier [20]. All experiments on human tissues were conducted with the authorisation of the Ethical Committee of the University of Debrecen, as well as with the written consent of the patients. The tissue samples employed in the present study were surgically removed for postoperative histopathological diagnosis. After removal, the tissue specimens were immediately fixed in 4% buffered formaldehyde (24 h), embedded in paraffin wax, and 4-μm-thick sections were cut.

For AR, the tissue sections were either incubated in 8 mM Tris buffer pH 8.4 for 15 min in a microwave oven (750 W) or they were subjected to high temperature at high pressure (in a pressure cooker) for 2 min (in 0.1 M citrate buffer pH 6.0). In the next step, the endogenous peroxidase activity was blocked with 3% H_2O_2 in methanol (10 min, room temperature). Non-specific binding was prevented by incubating the sections with Protein Block Serum Free Reagent (DAKO, Glostrup, Denmark; 5 min, room temperature). The tissue sections were then incubated overnight at 4 °C with one of the anti-TASK-3-specific primary antibodies. Two antibodies were polyclonal [raised in goat (Santa-Cruz Biotechnology Inc., Santa Cruz, CA, USA) or rabbit (Alomone Labs. Ltd., Jerusalem, Israel)], whereas the third antibody was the newly developed monoclonal antibody. The antibody dilution ranges were 1:100–1:1000; 1:800–1:2000 and 1:200–1:2000, respectively. The antibody raised in rabbit targeted an epitope of the TASK-3 channel protein close to its N terminus, whereas the other two antibodies recognised epitopes near to the C-terminal region.

After incubation, the slices were rinsed in PBS (0.02 M NaH_2PO_4, 0.1 M NaCl, 3 × 5 min). If the primary antibodies were raised in rabbit or mouse, the tissue sections were incubated with the EnVision system (DAKO) visualised by employing VIP SK4600 kit (Vector Laboratories, Burlingame, CA, USA). If the primary antibody was raised in goat, the sections were incubated in biotinylated anti-goat secondary antibodies (raised in rabbit) for 30 min (1:100, DAKO), then rinsed with PBS (3 × 5 min) and incubated with horseradish peroxidase-conjugated streptavidin (30 min; 1:500; room temperature). In these instances visualisation of the immunolabelling was also achieved using VIP. At the end of the procedure slight counterstaining was performed using methyl green.

Control experiments were regularly performed. In these cases, the polyclonal antibodies were co-incubated with the antibody-specific blocking peptides (supplied by the manufacturer of the primary antibody), according to the instructions provided by the supplier. When the monoclonal antibody was employed, control experiments were completed by leaving the primary antibody out of the reaction. The control experiments were always conducted after the application of one of the AR techniques.

Cell cultures. Three established melanoma cell lines [26] were employed in the present work, namely WM35 (a human melanoma cell line from a primary, radial growth phase tumour site), HT199 and HT168-M1 (the latter two are metastatic human melanoma cells). HT168-M1 is a derivative of the A2058 human melanoma cell line: the A2058 cell line was adapted to *in vivo* growth as xenograft, establishing the HT168 cell line. After intrasplenic transplantation of HT168 cells into immunosuppressed mice, a highly metastatic variant (HT-168-M1) was selected. The cells were cultured in RPMI 1640 medium supplemented with 10% foetal bovine serum (FBS), 2 M L-glutamine, 50 U/ml penicillin, 50 μg/ml streptomycin and 1.25 μg/ml fungizone (Biogal, Debrecen, Hungary). C2C12 cells (an immortalised mouse skeletal muscle cell line) were cultured in DMEM medium containing 10% FBS, 50 U/ml penicillin, 50 μg/ml streptomycin and 1.25 μg/ml fungizone. The cell lines were maintained as monolayer cultures in T75 flasks and they were kept in a 5% CO_2 atmosphere at 37 °C; feeding was performed on every other day. Cells were passaged at 80–100% confluence (about every 6–7 days). All chemicals were purchased from Sigma-Aldrich, unless indicated otherwise.

Immunocytochemistry. Prior to the immunocytochemistry, the melanoma cells were first gently fixed in 4% paraformaldehyde (15 min, room temperature), and rinsed in PBS containing 100 mM glycine (3 × 5 min). Permeabilisation was achieved by applying PBS containing 0.1% Triton X-100 (10 min); the cells were then rinsed in PBS (3×). Blocking was performed with PBS containing 1% BSA for 30 min at room temperature, followed by the application of the primary antibodies (4 °C, overnight). On the following day, the cells were rinsed in PBS (3×), incubated with the secondary antibodies for 1 h at room temperature and washed with PBS (3×). Finally, the melanoma cells were mounted using Vectashield mounting medium containing DAPI (Vector).

When immunopositivity for HMB-45 and S-100 protein was investigated, the major steps of the procedure were as described above. Mouse monoclonal anti-HMB-45 (1:50; DAKO) and rabbit polyclonal anti-S-100 (1:500; LabVision, Fremont, California, USA) antibodies were applied.

Control experiments were regularly performed. In these cases the polyclonal antibodies were co-incubated with

the antibody-specific blocking peptides (supplied by the manufacturer of the primary antibody), according to the instructions provided by the supplier. When monoclonal antibodies were employed (either anti-TASK-3 or anti-HMB-45), control experiments were performed leaving out the primary antibody.

Microscopy. All the non-fluorescent and some of the fluorescent immunoreactions were investigated using a Nikon Eclipse 600W microscope (Nikon, Tokyo, Japan), equipped with an RT colour CCD camera. The images were acquired using the Spot RT v3.5 software.
In other cases, the fluorescent labelling was assessed using a laser scanning confocal microscope (Zeiss LSM 510 microscope; Oberkochen, Germany) with a 40× oil-immersion objective. In some instances, 10–25 'Z-stack' images were obtained from the areas or cells of interest, the thickness of the individual optical sections varied between 0.5 and 1.0 µm. The reconstruction of the images was performed using the Zeiss LSM Image Browser. The final forms of the illustrations were created using Adobe Photoshop 7.0.

Transient transfection of C2C12 cells. Naïve C2C12 cells were found not to possess noteworthy TASK-3 immunopositivity, making them ideal candidates for the transfection experiments. C2C12 cells were transfected with a human TASK-3-encoding plasmid (pcDNA3 hTASK3/7; a kind gift from Prof. Peter R. Stanfield and Dr. Ian Ashmole). The TASK-3 cDNA was blunt end cloned into the EcoRV site of the vector pcDNA3 (Invitrogen, Carlsbad, CA, USA). Transient transfection was performed on cells seeded onto coverslips with Superfect transfection reagent (Qiagen, Hilden, Germany) according to the instructions provided by the manufacturer. Plasmid DNA (2 µg) was applied onto each coverslip. After the transfection, cells were allowed to express the introduced gene for 48 h in 5% CO_2 atmosphere at 37 °C. Immunocytochemistry was performed as described for the melanoma cells.

Generation of a stably transfected HEK293 cell line. Human embryonic kidney (HEK293) cells were continuously cultured in a Dulbecco's Modified Eagle Medium (DMEM) complemented with 10% FBS, 1% MEM non-essential amino acids, 50 U/ml penicillin, and 50 µg/ml streptomycin and were incubated at 37 °C in a humidified incubator with 5% CO_2/95% O_2. PCR product corresponding to the full-length coding sequence of TASK-3 channel was ligated into the pIRES expression vector (Clontech Laboratories, Cowley, UK). Following transformation of competent *E. coli*, colonies were selected, cultured and sufficient quantities of plasmid DNA were produced with a Plasmid Maxi Kit (Qiagen Ltd., Crawley, UK). Transfection was performed using a mix of linearised plasmid DNA with calcium phosphate (Promega, Southampton, UK) for 30 h to allow expression of the transferred gene. Subsequently, the medium was changed to a high potassium (25 mM) growth medium containing the selecting agent neomycin (800 µg/ml).

Preparation of nuclei. The nuclear fraction from melanoma cell cultures was isolated using modifications of previously described protocols [27, 28]. Two methods were employed for harvesting the cells: they were either scraped mechanically, or they were trypsinized. In the former case the cells were gently scraped in ice-cold PBS and centrifuged (1000 *g*; 10 min, 4 °C); the pellet was collected and resuspended in Buffer A [10 mM HEPES; 1.5 mM $MgCl_2$; 10 mM KCl; 0.1 mM EDTA; 0.1 mM EGTA; 1 mM dithiothreitol; 0.5 mM phenylmethylsulfonyl-fluoride; protease inhibitor cocktail (Sigma-Aldrich), pH 7.4]. In the latter case, the cells were trypsinised, and growth medium containing 10% FBS was added. The cells were collected by centrifugation at 1000 *g* for 5 min, washed twice in ice cold PBS and resuspended in Buffer A. The application of both harvesting techniques gave the same results.
The cells were left to swell on ice for 20 min, and Nonidet P-40 was added (final concentration, 0.5%); the cells were lysed in a Dounce homogeniser by repeated strokes. The extent of lysis was monitored by staining 10 µl lysate with trypan blue. The ratio of lysed cells was over 90%. The lysate was centrifuged at 770 *g* for 10 min at 4 °C to yield a crude nuclear pellet. The pellet was resuspended in 2.2 M sucrose Buffer A and centrifuged at 40 000 *g* for 90 min at 4 °C. The pellet was washed twice, dissolved in 0.25 M sucrose in Buffer A and sonicated. The protein content of the nuclear fraction was determined using a BCA-kit (BCA™ Protein Assay Kit, Pierce, Rockford, IL, USA), then stored at –70 °C.

Western blotting. Both total cell lysates and nuclear fraction were employed for the Western blot experiments. When total cell lysates were prepared, the cells were washed three times with ice-cold PBS and scraped in 100 µl lysis buffer [20 mM Tris-HCl, 5 mM EGTA, 1 mM 4-(2-aminoethyl) benzenesulphonyl fluoride, 20 µM leupeptin, pH 7.4] on ice. The suspension was sonicated on ice, and protein concentration was assessed with the BCA-kit.
For the Western blot experiments, a procedure described earlier [20] was slightly modified. Total cell lysates or the nuclear fractions were mixed with SDS-PAGE sample buffer and boiled for 10 min at 100 °C. The samples were subjected to SDS-PAGE [7.5% gels were loaded with 160 µg (whole cell preparation) or 50 µg (nuclear fraction) protein per lane] and transferred to nitrocellulose membranes (Bio-Rad Laboratories, CA, USA). The nitrocellulose-bound proteins were visualized by staining with Ponceau S and were then blocked with 5% dry

milk in PBS supplemented with 0.05% Tween20 (PBST) and probed with one of the TASK-3-specific primary antibodies (Alomone, 1:800). The secondary antibody was horseradish peroxidase-conjugated goat anti-rabbit IgG antibody (Bio-Rad, 1:1000). In control experiments, specificity of staining was assessed by incubating the membrane with the primary antibody preincubated with its specific blocking (immunising) peptide, a procedure that completely prevented the immunosignal in all cases. The immunoreactive bands were visualised using an enhanced chemiluminescence Western-blotting detection kit (Pierce), in a Fuji film Labs-3000 dark box (Tokyo, Japan).

Electrophysiology. Measurement of the K^+ current passing through the TASK-3 channels present in the cell surface membrane of transfected HEK cells was recorded using the whole-cell configuration of the patch-clamp technique. Patch-clamp pipettes were fabricated from borosilicate glass capillaries (Clark Electromedical Instruments, Reading, UK), and filled with a solution containing 140 mM KCl, 10 mM HEPES, 4 mM $MgCl_2$, and 10 mM EGTA, pH 7.3. The resistance of the patch pipettes varied between 2 and 4 MΩ. The current was recorded by employing an Axopatch 200B patch-clamp amplifier connected to a DigiData 1200 interface (Axon Instruments, Foster City, CA). Data acquisition and analysis were performed using the pClamp 6.0 software. To assess the pH sensitivity of the current, the regular extracellular solution (130 mM NaCl, 5 mM KCl, 2 mM $CaCl_2$, 1 mM $MgCl_2$, 15 mM HEPES, 30 mM glucose, pH 7.4) was replaced with a bathing solution with similar composition but with a more acidic pH (pH 6.0).

Construction of a TASK-3-pEGFP. The TASK-3 cDNA was amplified by PCR with the oligonucleotide primers 5′-GTTAATTGAATTCATGAAGAGGCAGAACGTGCG-3′ (sense) and 5′-GTTATAAAGGATCCAACTGACTTCCGGCGTTTCA-3′ (antisense). The PCR was performed using 1 cycle of 95 °C for 5 min, 35 cycles of the sequence of 95 °C for 1 min, 60 °C for 30 s, 72 °C for 3 min, and finally 1 cycle of 74 °C for 3 min. The product was purified using QIAquick PCR purification column (Qiagen). The amplified product was digested with *Eco*R1 and *Bam*H1 then ligated into *Bam*H1- and *Eco*R1-digested pEGFP-N1 (Clontech Laboratories) to generate the TASK-3-pEGFP fusion vector. JM 109 competent *E. coli* were transformed with the newly constructed plasmid, and clone selection was achieved using 30 μg/ml kanamycin on LB agar. After selection, the plasmid was isolated using Wizard® Plus SV Miniprep DNA purification Kit (Promega). The newly constructed fusion vector was verified by DNA sequencing.

Results

TASK-3 immunopositivity of formalin-fixed, paraffin-embedded melanoma sections. As demonstrated in Figure 1A and B, the melanoma tissue sections demonstrated strong TASK-3-specific immunolabelling, regardless of the type of antibody tested (although the intensity of the immunopositivity was somewhat weaker in the case of the monoclonal antibody), whereas immunopositivity was never seen in the connective tissue. Preadsorption control experiments were regularly performed, and neither the tissue section presented in the inset of Figure 1A,

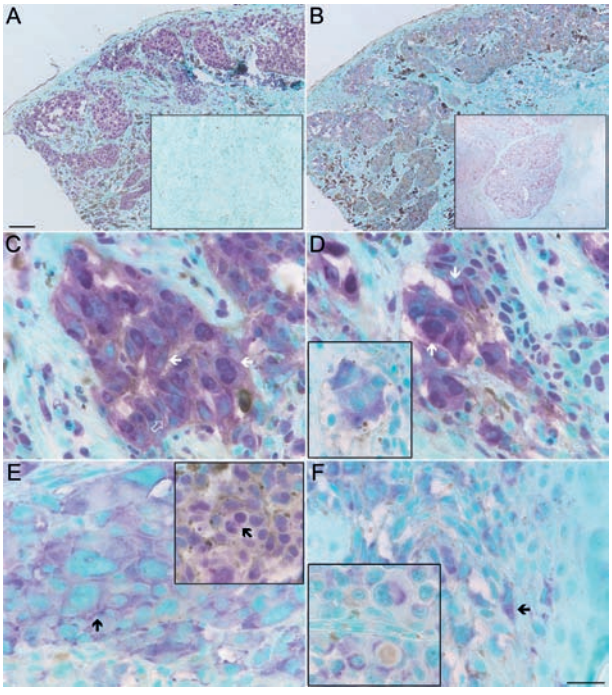

Figure 1. TASK-3-specific labelling of formalin-fixed histopathological tissue sections obtained from primary and metastatic melanomas. (*A*) Application of a polyclonal antibody (Alomone Labs Ltd.) after completing the antigen retrieval (AR) with citrate buffer. Inset shows the result of a preadsorption control experiment. (*B*) Application of the monoclonal antibody after completing the AR with Tris buffer incubation. Inset shows the immunoreaction performed on a tissue section excised from metastatic melanoma of the small intestine. (*C*) Immunoreaction using a polyclonal antibody (Alomone Labs Ltd.; Tris incubation). Filled arrows indicate surface membrane labelling of cells, open arrow shows a cell whose process demonstrates strong TASK-3-positivity. (*D*) In the main panel the same antibody and AR were employed as in (*A*), in the inset, monoclonal antibody was used (after Tris incubation). In the main panel arrows indicate cells with intense perinuclear labelling; this phenomenon is also obvious in the inset. (*E*) Immunoreactions after applying the polyclonal antibodies (main panel: Santa Cruz Biotechnology Inc., citrate incubation; inset Alomone Labs Ltd., Tris incubation). In the main panel arrow shows a cell with prominent intense perinuclear immunopositivity. In the inset, the arrow indicates a cell with a reticular distribution of labelling between the nuclei. (*F*) Immunoreactions obtained using the monoclonal antibody (Tris incubation). Arrow indicates a cell with an obvious purple, granular pattern of immunopositivity. Bars A, B 100 μm; C–F 25 μm.

nor other tissue specimens treated with preadsorbed primary antibodies showed appreciable immunopositivity. TASK-3 immunopositivity was observed in metastatic melanomas (inset of Fig. 1B).

Figure 1C–F summarises the results of the TASK-3-specific immunoreactions when investigated at higher magnification. All three primary antibodies produced reliable labelling of the melanoma cells. Although the immunopositivity occasionally seemed to be associated with the cell surface (see the cells indicated by white arrows in Fig. 1C), in most of the cases the strongest labelling was seen intracellularly, often giving a granular pattern (Fig. 1F). A prominent perinuclear distribution of immunopositivity was frequently seen (Fig. 1E, F); in the cases of tumourous giant cells or dividing forms, strong immunopositivity was often situated between the individual nuclei (inset in Fig. 1E). In some cases the immunoreaction was strongest at one of the poles of the nucleus (Fig. 1D and inset of F). The observable processes of the melanoma cells also showed immunopositivity (see the cells indicated by the oblique and black arrows in Fig. 1C and E, respectively). Although the general pattern of the labelling was the same for all three primary antibodies tested, there was a certain difference in terms of the nuclear labelling: the antibody purchased from the Alomone gave the strongest nuclear reaction (although clearly negative nuclei were also observed; see Fig. 1C, 1D and E inset), whereas the nuclear positivity was less pronounced when the other two primary antibodies were utilised (Fig. 1E, F).

Altogether 14 melanoma tissue samples (7 primary, melanotic, skin melanomas and 6 metastatic ones) were investigated in the frame of the present study and the distribution of the immunopositivity was very similar to those presented in Figure 1 in each case. The intensity of the reaction was strong (assessed as ++++ or +++) in 10 out of the 14 investigated melanoma sections, in 3 cases it was somewhat weaker (++), whereas in one metastatic melanoma sample the immunopositivity was present but hardly detectable (+). Although neither the total number of samples nor the limited diversity of the tumour sections (all the primary tumours corresponded to Clark IV or Clark V stages) available permitted a comprehensive analysis of the possible alterations of the TASK-3 expression patterns of the melanoma tissue samples, no obvious differences were seen in the characteristics of the immunopositivity (*i.e.* ratio of the labelled nuclei, intensity of the reaction) amongst the individual cases.

TASK-3 immunopositivity of formalin-fixed, paraffin-embedded benign naevus sections. As the presence and function of the TASK-3 channels are thought to be associated with the genesis of certain malignant tumours, we investigated whether TASK-3 immunopositivity was a unique feature of the melanoma cells, distinguishing them from healthy melanocytes, or whether the melanocytes also possessed noticeable TASK-3 immunopositivity. As demonstrated in Figure 2, most melanocytes showed distinct and strong TASK-3 positivity, with all three primary antibodies tested. The labelling often gave a clearly granular pattern (Fig. 2A–C, arrows). Similarly to the melanoma tissue specimens, the labelling was not prominent without AR (not shown), whereas the application of one of the AR methods greatly enhanced the intensity of the immunoreaction. The distribution pattern of the labelling was essentially the same as in the melanoma sections (intense perinuclear labelling; see the cell indicated by arrow in Fig. 2C). Similarly to the melanoma sections, the nuclear polymorphism (the presence of labelled as well as unlabelled nuclei) was also noted in tissue sections obtained from benign moles. The preadsorption control experiments did not result in noticeable immunopositivity (Fig. 2D). Similar experiments were carried out on tissue samples excised from four different nevi, with similar results.

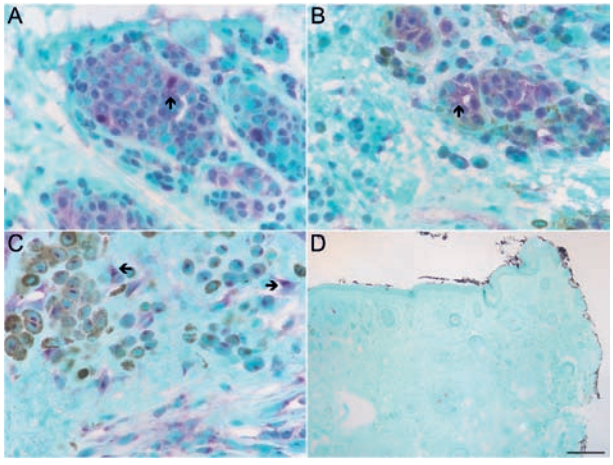

Figure 2. TASK-3-specific labelling of benign moles. (*A*) Immunolabelling obtained using polyclonal antibody (Alomone Labs Ltd., citrate incubation). Arrow indicates a cell showing prominent, granular immunolabelling. (*B*) Immunolabelling obtained using polyclonal antibody (Alomone Labs Ltd., citrate incubation). Arrow indicates a naevus cell whose process demonstrates intense TASK-3-specific labelling. (*C*) Immunoreaction obtained using the other polyclonal antibody (Santa Cruz Biotechnology Inc., Tris incubation). Arrows indicate cells with strong, intracellular labelling. (*D*) The result of a preadsorption control experiment (Alomone Labs Ltd., Tris incubation). Bar A–C 25 μm; D 375 μm.

TASK-3 immunopositivity of human melanoma cells maintained in cell culture. The investigation of the TASK-3 expression of the melanoma cells in tissue samples clearly indicated that they possessed TASK-3 positivity. However, although formaldehyde-fixed tissue samples are appropriate for the investigation of the presence and distribution of the TASK-3 immunolabelling, they cannot be used for functional experiments, which

– on the other hand – would be essential for the more detailed investigation of both the functional relevance of the TASK-3 channels, and the consequences of the manipulation of these channels. As such experiments are most conveniently performed on melanoma cells maintained in cell culture, in the next step of the experiments TASK-3 immunopositivity of the cultured melanoma cells was investigated.

Three cell lines were employed for the immunocytochemical experiments (see Materials and methods). The identity of the cells in the tissue culture was confirmed by demonstrating their S-100 protein and HMB-45 positivities (not shown). The homogeneity of the cultures was assessed by determining the ratios of the HMB-45 positive and negative cells in all three cell lines. The proportion of the non-HMB-45-positive cells was so low [HMB-45-positive cells: 97 ± 2; 93 ± 3 and 95 ± 4% for the primary (n = 630) and the two metastatic cells lines (n = 1345 and n = 1137), respectively; average ± SD] that their presence did not disturb either the immunocytochemical or the Western blot experiments.

All types of TASK-3-specific primary antibodies gave strong and consistent immunopositivity when tested on either primary or metastatic melanoma cell lines (not shown), although when switching to higher magnifications (Fig. 3) there were some differences between the intracellular labelling patterns produced by the individual primary antibodies. The antibody targeting the epitope near the N terminus of the channel gave more intense nuclear-perinuclear reaction, whereas the other two primary antibodies (recognising epitopes near the C terminus of the peptide chain) produced less prominent (but definitely present) nuclear-perinuclear positivities (compare Fig. 3A, D, F with B, E). On the other hand, antibodies recognising the N terminus gave particularly rich and complex patterns of intracellular positivity (see the confocal image demonstrated in the inset of Fig. 3A). Although this seemed to be less pronounced in case of the antibody specific for the epitope near the N terminus of the protein (especially when investigating the results with conventional fluorescent microscopy), confocal microscopy clearly revealed that the rich intracellular labelling was also present in these instances (Fig. 3G). Regardless of the primary antibody employed, however, the cytoplasmic reaction always seemed to concentrate around or at one pole of the nucleus, and (in case of polynuclear cells)

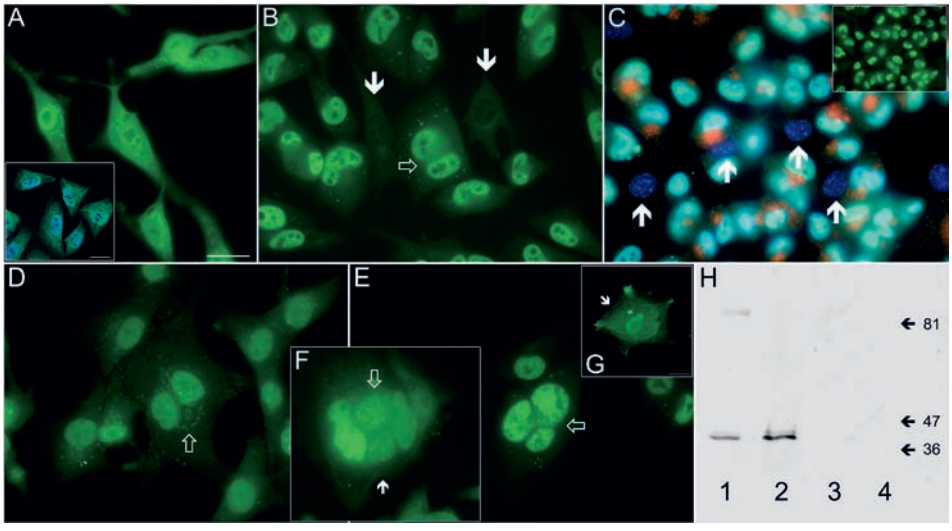

Figure 3. High magnification view of the TASK-3-specific immunolabelling of the melanoma cell lines. (*A*) Application of monoclonal antibody (WM35 cell line). Distinct reticular pattern of the immunopositivity is most prominent in the proximity of the nuclei, which is particularly obvious using confocal microscopy (inset: nuclei are visualised by their DAPI labelling). (*B*) Application of polyclonal antibody (Alomone Labs Ltd.) on the cell line HT199. Open arrow indicates a cell with immunopositivity between the nuclei. Filled arrows show the positions of two cells demonstrating no TASK-3 labelling. (*C*) TASK-3 (Alomone Labs Ltd.) and HMB-45 double labelling of the HT199 cell line combined with DAPI labelling of the nuclei. Arrows indicate cells whose nuclei are clearly seen but do not demonstrate either TASK-3- or HMB-45-positivity. Inset shows the result of the TASK-3-specific labelling of the same visual field. (*D*) Application of polyclonal antibody (Santa Cruz Biotechnology Inc.) on the cell line WM35. Arrow indicates the strong, reticular pattern of the labelling between and around the cell nuclei. (*E*) Application of polyclonal antibody (Alomone Labs Ltd.) on the cell line WM35. Arrow indicates the strong labelling between the nuclei. (*F*) Application of monoclonal antibody on the cell line HT199. Open arrow indicates the strong, reticular immunopositivity pattern in the proximity of the nuclei; filled arrow points to a portion of the cell with immunolabelling of the cell surface membrane. (*G*) Application of polyclonal antibody (Alomone Labs Ltd.) on the cell line WM35, viewed with confocal microscopy. Arrow indicates a portion of the cell with cell surface membrane immunopositivity. Bars 25 µm. (*H*) Western blot conducted using a polyclonal antibody (Alomone Labs Ltd.). Lane 1: Total cell lysate (160 µg protein); lane 2: nuclear fraction (50 µg protein). Lanes 3 and 4: same but primary antibody was co-incubated with its specific blocking peptide. The numbers on the right indicate the positions of the molecular weight standards (kDa).

between the nuclei, giving the appearance of a 'meshwork' (hollow arrows in Fig. 3B, D–F). In some cases the immunolabelling was clearly associated with the surface membrane (filled arrows in Fig. 3F, G).

The dividing cells showed more intense TASK-3 labelling in all three cell lines tested than the neighbouring, not dividing ones. The immunopositivity was present in the entire cytoplasm in these dividing cells, showing an intense and rather homogeneous appearance. In the cells just completing cell division, the TASK-3 immunopositivity was usually concentrated in between or just around the newly formed nuclei. In two cases, WM35 cells were maintained in 1% serum for 24–48 h (similar to the method described by Pei et al. [18]) to investigate how this manoeuvre altered the TASK-3 immunopositivity pattern. Although neither the distribution of the TASK-3-specific labelling, nor the proportion of the TASK-3-positive nuclei changed significantly, the intensity of the immunopositivity increased compared with that observed in control melanoma cells.

It is worth noting that some of the cells situated in the tissue culture did not show anti-TASK-3 immunopositivity (cells indicated by arrows in Fig. 3C). As seen in Figure 3C, the cells with no TASK-3 positivity were the ones that did not present melanoma-specific markers (in the present case no HMB-45 positivity could be observed).

Western blot experiments. The results of the immunohistochemical and immunocytochemical experiments indicated that all three primary antibodies labelled the same structures and the same cells, with some differences in the relative intensities of the various subcellular structures (cytoplasmic *vs*. nuclear-perinuclear reactions). Although it seemed to be very unlikely that all three primary antibodies produced the same distribution of a non-specific labelling, to provide further evidence of the validity of the immunoreactions, Western-blot experiments were conducted using protein samples prepared from melanoma cell cultures. Figure 3H shows a representative example of such experiments. As shown, the total protein preparation resulted in two distinct bands (lane 1), corresponding to the monomer and dimer forms of the channel. Neither band was observed if the primary antibody was preincubated with its specific blocking peptide (lane 3). Moreover, the nuclear fraction from the same culture gave a strong, specific band appeared at the position corresponding to the human TASK-3 channel monomers (lane 2). The preadsorption control experiments did not result in positive labelling (lane 4), further confirming the specificity of the immunoreaction.

TASK-3 immunopositivity of the rat zona glomerulosa and of transfected C2C12 and HEK cells. The results presented so far suggested that the melanoma cells possessed strong TASK-3 immunopositivity. However, the rich intracellular labelling and the relatively sparse cell surface membrane positivity were somewhat surprising. It seemed to be logical, therefore, to check whether positive immunolabelling could be obtained in a tissue section where the presence and activity of the TASK-3 channels had been already functionally demonstrated on the surface membrane. The most obvious selection was the rat adrenal gland, for which the prominent role of the TASK-3 channels controlling aldosterone secretion had been convincingly demonstrated previously [29]. The experiments on the rat adrenal gland sections were performed using the polyclonal antibody recognising the epitope near the N terminus of the channel, as this antibody had confirmed rat TASK-3 channel specificity. As the low magnification part of Figure 4A demonstrates, intense immunolabelling was observed in the most superficial part of the adrenal gland, corresponding to the aldosterone producing zona glomerulosa. Less intense, but clearly present positivity was also noted in the adrenal medulla. In contrast, neither the connective tissue encapsulating the adrenal gland (Fig. 4B), nor the other two layers of the adrenal cortex (Fig. 4A) demonstrated considerable TASK-3 positivity. Higher magnification (Fig. 4B, C) revealed that the cell nuclei of the otherwise strongly labelled rat zona glomerulosa cells showed no TASK-3 positivity at all. Moreover, importantly, the cell membrane demonstrated strong and definite TASK-3 labelling. Positive labelling was also seen in the cytoplasm of the cells, and in some cases it showed a clearly granular distribution. Therefore, the antibody used in this experiment was capable of recognising the TASK-3 channels in the cell membrane (and in the cytoplasm), suggesting that the relatively weak surface membrane positivity observed in human melanoma cells was not the consequence of the inadequacy of the primary antibodies, but indicated the low quantity of these channels there.

In the next set of experiments, cell lines that were TASK-3 negative were transfected with TASK-3 channel coding vectors (both stable and transient transfection systems were employed) and analysed to confirm that all three primary antibodies recognised the appropriate channel protein. As shown in Figure 4D–F, strong immunpositivity was observed in those C2C12 cells where the transfection was successful; and the close proximity of the non-transfected cells provided convenient intrinsic negative controls of the reaction. As demonstrated, the immunolabelling of the successfully transfected C2C12 cells showed a rich, reticular, cytoplasmic distribution (similar to the results of Callahan et al. [30]) without obvious nuclear reaction. No positively labelled cells were observed in the mock-transfected C2C12 cell cultures.

Stably transfected HEK cells were also employed, and representative results of their TASK-3-specific immunolabellings are presented in Figure 4I and J. As shown, strong immunopositivity was observed in the cytoplasm,

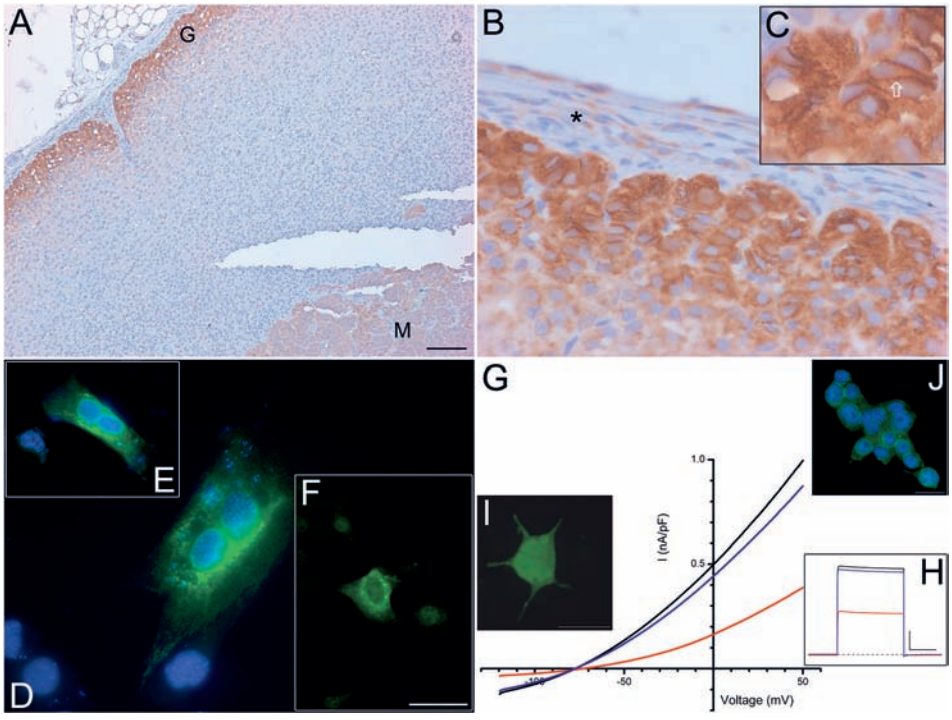

Figure 4. Positive control experiments assessing the applicability of the primary antibodies. (*A*) Low magnification view of an immunoreaction conducted on tissue sections excised from formalin-fixed rat adrenal gland using a polyclonal antibody (Alomone Labs Ltd.). Intense immunopositivity is present in the zona glomerulosa of the adrenal cortex (*G*) along with a somewhat weaker but clear labelling of the adrenal medulla (*M*). (B, C) High magnification views of the TASK-3 labelling of the rat zona glomerulosa. The immunopositivity is clearly present in the cell surface membrane (see arrow in C). The connecting tissue encapsulating the adrenal gland (*) does not show noteworthy labelling. Bars 100 µm (*A*), 25 µm (*B*) and 12.5 µm (*C*). (D–F) TASK-3 labelling of transiently transfected C2C12 cells. (D, E) Monoclonal antibody was applied (co-localisation images with the result of the DAPI labelling); whereas (*F*) shows the situation after applying polyclonal antibody (Alomone Labs. Ltd.). Cells that were not transfected seen in the proximity show no or very faint immunopositivities. Bars 25 µm (D, F) and 37.5 µm (*E*). (G, H) Functional demonstration of the TASK-3 channels in the surface membrane of stably transfected HEK cells. (*G*) Cells were held at –80 mV, and a 800-ms ramp protocol was applied from –120 mV to +50 mV (corresponding to a membrane potential change of 0.2125 V/s). The protocol was repeated in every 3 s, and the averages of five traces are shown. The control, pH 7.4, is presented in black; the current trace recorded in a more acidic extracellular solution, pH 6.0, is red; the blue trace represents the result of the wash-out. (*H*) The cell was held at –80 mV, then a pre-pulse potential was applied to –90 mV for 200 ms, followed by a depolarisation to +30 mV for 600 ms. Currents appearing during the depolarisation are plotted (black: control; red: pH 6.0; blue: wash-out). Bar 3 nA and 200 ms. (I, J) TASK-3-specific immunolabelling using (*I*) a polyclonal antibody (Alomone Labs Ltd.) (composite confocal view), and (*J*) monoclonal antibody (co-localisation with DAPI) on stably transfected HEK cells. Bars 25 µm.

but it also appeared in the surface membrane (Fig. 4J). Preadsorption control experiments conducted on the stably transfected HEK cells did not result in appreciable labelling (not shown).

Functional measurements were also made for transfected HEK cells, and the results of these trials are shown in Figure 4G and H. As seen in Figure 4H, when the transfected HEK cells were subjected to depolarisation, a large outward current appeared, which could be effectively blocked by extracellular acidification. As indicated, the inhibitory effect of shifting the extracellular pH from 7.4 to 6.0 proved to be reversible. When a suitable ramp protocol was applied, a current could be recorded which reversed near the calculated equilibrium potential of K^+ (Fig. 4G). When the same protocol was repeated in a more acidic extracellular solution (pH 6.0), the current was strongly inhibited, without changing its reversal potential. The effect of acidic extracellular pH on the current evoked by depolarising ramp protocols could also be effectively reversed.

Distribution of a TASK-3-GFP fusion protein in the melanoma cells. One of the most surprising discoveries of the present experiments was the finding that the TASK-3 channel protein seems to appear in the nucleus of the melanoma cells. Although the immunocytochemistry and immunohistochemistry data, along with the results of he Western-blot experiments, indicated that this observation was not an artefact, one more test was performed to see whether the channel protein could enter the nuclei of the cells. In these experiments the melanoma cells were transfected with a newly constructed TASK-3-GFP-encoding plasmid, and the distribution of the fluorescent protein was tested 2–3 days after the transfection. As

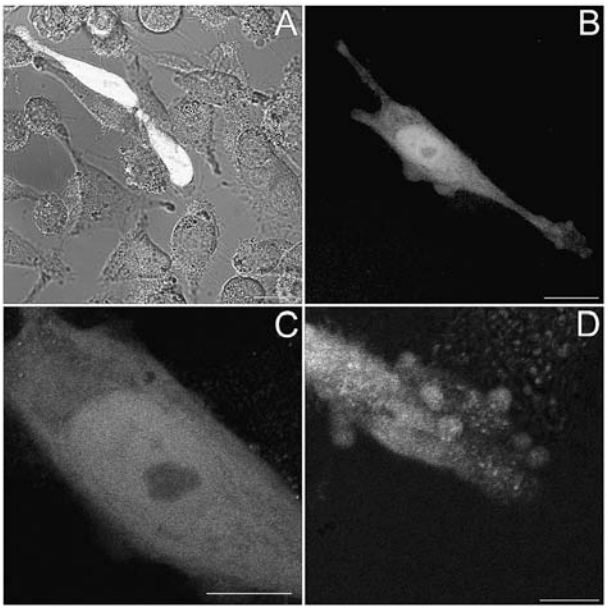

Figure 5. Distribution of a TASK-3-GFP fusion protein in melanoma cells maintained in cell culture. (*A*) Differential interference contrast view of melanoma cells (WM35) maintained in cell culture superimposed with the fluorescent image of the same visual field showing the presence of the TASK-3-GFP fusion protein in the successfully transfected cells. (*B*) Intracellular distribution of the TASK-3-GFP fusion protein in a melanoma cell. Composite image of seven individual sections (z = 1 μm). (*C*) High magnification view of the same cell demonstrating its nuclear region. (*D*) High magnification view of the same cell showing the end of the lower process (as seen in B). Bars A, B 20 μm; C 10 μm; D 5 μm.

demonstrated in Figure 5A, the successfully transfected melanoma cells showed intense fluorescence. Moreover, the distribution of the green fluorescence (Fig. 5B) was similar to that observed in the immunocytochemistry experiments (Fig. 3A); the fluorescent signal was present in the cytoplasm, it could be clearly observed in the nucleus (but it spared the nucleolus; Fig. 5C), and it concentrated in the terminal regions of the processes (Fig. 5B, D).

Discussion

In the present study, three different TASK-3-specific antibodies (a newly developed monoclonal and two polyclonal) were employed to assess the TASK-3 expression of melanoma cells both in formalin-fixed, wax-embedded tissue sections and in cultures using immunocytochemistry. The specificity of the primary antibodies was confirmed by functional, Western-blot, and heterologous expression experiments. Melanoma cells proved to be strongly positive for TASK-3, regardless of the primary antibody used. Strong intracellular positivity was observed that seemed to be associated with the nuclear envelope and other intracellular membranes. The data presented indicate that neither the presence nor the distribution pattern of the TASK-3-specific labelling differs in malignant melanoma cells and in benign melanocytes, thus TASK-3-specific labelling cannot distinguish between a benign mole and a malignant melanocytic tumour.

Possible roles of TASK-3 channels under physiological and pathological circumstances. TASK-3 channels are ubiquitously present 'background' K^+ channels. The molecular composition, biophysics and pharmacology of these channels have been thoroughly studied in the past few years, but (for obvious reasons) mostly in heterologous expression systems and in animal tissues. There are a number of physiological functions related to the activity of TASK-3 channels: they are responsible for the acidosis and hypoxia sensitivity of both the peripheral and central chemoreceptors [23, 31–34], and have important roles in the regulation of aldosterone secretion in the zona glomerulosa cells of the adrenal medulla [29]. They may have significance in the mediation of short- and long-term changes of neuronal excitability [1, 35–41], they may be involved in the neurone-glia interaction [42], and they may regulate cell apoptosis ([15, 16]; for a review see [43]). The significance of TASK-3 channels has also been implied in a number of pathological situations and conditions. Since they are activated by certain volatile general anaesthetics and their activity results in membrane hyperpolarisation and reduced excitability, they may mediate the effects of halothane and isofluorane [14]. Moreover, along with that of the TASK-1 channels, their activation may also be responsible for the reduced ventilatory drive observed under general anaesthesia as their activation by the volatile compound hyperpolarises the chemoreceptor cells, making them less sensitive to either hypoxia or acidosis [44, 45]. It has also been demonstrated that the activity of TASK channels may provide protection for apoptosis and neuronal death [16]. TASK-1, TASK-2, and TASK-3 channel activation could all prevent apoptosis of C8 cells maintained in tissue culture; but only TASK-3 channels could do so in brain slices. The neuroprotective effect of TASK-3 channel activity may also explain why isofluorane application reduces neuronal cell death.

Although TASK-3 channel activity may induce apoptosis (in the case of cerebellar granule cells, this seems to be an important mechanism controlling the number of surviving granule cells in the cerebellar cortex, [15]), under certain experimental conditions the presence and activity of TASK-3 channels may have the opposite effect. Namely, overexpression of TASK-3 channels could effectively reduce the TNF-induced cell apoptosis, whereas the non-K^+-permeable point mutant (TASK-3^{G95E}) did not have the ability to do so [18]. Although it is not clear why TASK-3 activity may either induce or prevent cell apoptosis, the fact that TASK-3 channels can promote cell survival seems to be important for their tumorigenic functions. This observation is corroborated by previous

reports about the amplification of kcnk9 gene and overexpression of the TASK-3 channel protein in certain malignant tumours [17].

So far, the presence of TASK-3-specific immunoreactivity has been reported in colorectal cancers, and gastric cancer [20, 46]. It has also been demonstrated that a cell line derived from lung cancer (Ben) overexpresses TASK-3 channels. Considering the potential significance of the TASK-3 channels in tumorigenesis, it seems reasonable to assume that a correlation might exist between the presence, quantity or distribution of TASK-3 channels and certain clinical, histological or biological properties of the tumours. To assess such correlation, an effective, reliable and specific anti-TASK-3 antibody is required. The newly developed monoclonal antibody utilised here seems to be a good candidate to perform the necessary experiments. In the presence of the appropriate AR technique, it gave good immunopositivity in all cases that were also positive with the polyclonal antibodies, thus it allows large-scale retrospective analyses to be performed on paraformaldehyde-fixed, waxed-embedded tissue sections.

Is the immunolabelling pattern observed here the consequence of specific binding? The distribution of TASK-3 immunopositivity reported in the present work was surprising. The labelling was particularly prominent intracellularly, where it gave strong reticular pattern, which often concentrated in the perinuclear region, and also seemed to associate with the nuclear envelope. The immunolabelling appeared to be very strong in the processes of the melanoma cells, both in cell culture and in wax-embedded tissue sections. Interestingly, the immunolabelling of the cell surface of the melanoma cells was not particularly strong. The relatively low intensity of the distinct surface membrane labelling observed in melanoma cells could have been interpreted as the inadequacy of the antibodies to recognise the TASK-3 channel protein. There are, however, several lines of evidence clearly contradicting this possibility: First, no distinct cell surface labelling could be seen with any of the applied primary antibodies, and it is rather unlikely that none of them recognises the channel protein against which they had been raised. Second, in expression systems where cells were transfected with TASK-3 channel protein encoding vectors, all antibodies gave intense positivity in the successfully transfected cells, and no labelling was observed in the controls. Third, in cells where the presence of functional TASK-3 channels has been reported (rat zona glomerulosa [29]; or the stably transfected HEK cells, where the presence and activity of TASK-3 channels was electrophysiologically confirmed as part of this study), the surface membrane showed clearly recognisable TASK-3 positivity. It is worth noting that the distribution of the TASK-3 positivity was very similar to that presented by Berg et al. [36] employing a different type of antibody, recognising the C terminus of the TASK-3 channel protein, further confirming the reliability of the data presented in this work.

It can be concluded, therefore, that all three antibodies recognise the TASK-3 channel protein, but it is equally important to verify their specificity. Obviously, the ultimate test of the primary antibodies employed here would be their application in a human TASK-3 knockout system. In the absence of such model, however, less effective methods should be attempted, which are not as powerful alone as the potential use of a knockout system, but their combination can be regarded as a possible way to confirm specificity. The following observations indicate the specificity of the immunolabelling demonstrated in this work. Three different primary antibodies, recognising three different epitopes of the TASK-3 channel protein gave very similar labelling patterns. Although the intensity of the labelling was somewhat different, no difference was observed in terms of the types of cells recognised. Given the facts that all three antibodies were raised in different species, and the preadsorption control experiments gave consistently negative results, the possible non-specific binding of the secondary antibody could also be ruled out. The transfection experiments and the use of positive control tissues (zona glomerulosa and human cerebellar sections [20, 22]) also pointed out the applicability of the antigens. It is worth noting that the TASK-3-specific labelling of the rat zona glomerulosa was possible as the identity between the human and rat TASK-3 channels is 94% over the first 250 amino acids, thus antibodies raised against an epitope near the N terminus of the channel are expected to be specific for both rat and human TASK-3 channels [3].

The specific labelling pattern observed in the tissue sections was also recognised as an indication of the specificity: none of the antibodies labelled the connective tissue, thus it served as an intrinsic negative control of the reaction. The rather specific intracellular pattern also indicated specific, rather than non-specific binding. The Western blot experiments also gave reliable results, indicating one or two bands (corresponding to the monomer and dimer proteins), whose presence could not be observed in the presence of the specific immunising peptide. Association of the labelling with the nuclear envelope was also confirmed by the Western blot experiments performed on a nuclear fraction, where the immunopositive band appeared at the expected molecular weight, and its appearance could be consistently blocked by the preincubation of the primary antibody with its specific blocking peptide. Finally, the similarity between the distribution of the TASK-3-GFP fusion protein and the immunochemistry results also confirmed the validity of the presented data.

What might be the explanation of the intense intracellular labelling? These lines of evidence convincingly

demonstrate that the labelling pattern reported here is not an artefact. What might be, therefore, the explanation of the rather intense cytoplasmic reaction observed in this study? Intense intracellular positivity in transfected cells has also been reported in other studies [30, 47], implying that the intense synthesis of the channel protein may result in this distribution pattern. This might suggest that intense TASK-3 channel production also occurs in melanoma cells; but why do they not seem to appear at the cell surface in large quantities? In a recent study it was demonstrated that the interaction between the adapter protein 14-3-3 and the TASK-3 channels is essential for the proper trafficking and translocation of the molecule [48]. In the case of the TASK-1 channel, the interaction required a pentapeptide motif at the extreme C terminus, and deletion of a single amino acid at the C-terminus of both TASK-1 and TASK-3 channels abolished binding to 14-3-3, resulting in the inappropriate translocation of the channel protein to the cell surface membrane and a significant reduction of the macroscopic current. It is an intriguing possibility that, while the TASK-3 channels of the melanoma cells are synthesised by the appropriate cellular machinery in large quantities, the individual channel proteins are not properly translocated, either due to lack of proper interaction with the 14-3-3 protein (*i.e.* as the result of a mutation affecting the 14-3-3 binding motif) or due to other, currently unknown reasons.

It may also be the case that certain tumour cells lack the necessary system(s) required for the translocation, which may (at least partially) explain why the current density is much less in the malignant melanoma or the Ben cells than in healthy ones (zona glomerulosa, cerebellar granule cells, etc.). It has been implied that the actual current density present in the appropriate cells may be the key in determining whether TASK-3 channels serve anti-apoptotic or pro-apoptotic function; thus, the presence and activity of the translocational machinery of the cells may also be a decisive factor.

It should also be noted that the intracellular localisation of TASK-3 immunopositivity is not entirely unusual. Such localisation has been reported for rat cerebellar and cochlear astrocytes [22], large intestinal mucosa, pancreatic islet cells [20], and in certain neurones of the rat central nervous system [30]. In the latter case, immunogold technique was employed and large quantities of the immunoreactive products were found in the Golgi apparatus, endoplasmic reticulum and intracellular organelles. It is most likely that the TASK-3 channels are also present in these structures of the melanoma cells. Moreover, on the basis of the observations made in cultured melanoma cells, it cannot be ruled out that TASK-3 channel proteins may be associated with the nuclear envelope and they may be present in the mitochondrial membrane. One cannot, therefore, exclude the possibility that the presence of TASK-3 channels in the membranes of intracellular organelles is a common feature for these cells, playing an important, yet unknown role in the cellular functions.

Acknowledgements. The authors are indebted to Mrs. E. Károlyi, Mrs. T. Kálmánczy and Mr. P. Pap for their professional work on the tissue sections and to Dr. N. Szentandrássy for his help in the patch-clamp experiments. The rat adrenal gland tissue blocks were kindly provided by Prof. P. Enyedi. The experiments presented here complied with the current laws of Hungary. The tissue samples were investigated with the approval and authorisation of the Ethical Committee of the University of Debrecen as well as with the written consent of the patients or their relatives. This work was supported by grants of the Hungarian Academy of Sciences (OTKA T-046067; T-049151; NK-61412); GVOP 3.2.1-04-0162/3.0; ETT 151/2006 and The Wellcome Trust. M.G. was an OTKA Postdoctoral Fellow.

1 Lesage, F. and Lazdunski, M. (2000) Molecular and functional properties of two-pore-domain potassium channels. Am. J. Physiol. 279, F793–F801.
2 Ashmole, I., Goodwin, P. A. and Stanfield, P. R. (2001) TASK-5, a novel member of the tandem pore K^+ channel family. Pflügers Arch. 442, 828–833.
3 Chapman, C. G., Meadows, H. J., Godden, R. J., Campbell, D. A., Duckworth, M., Kelsell, R. E., Murdock, P. R., Randall, A. D., Rennie, G. I. and Gloger, I. S. (2000) Cloning, localisation and functional expression of a novel human, cerebellum specific, two pore domain potassium channel. Brain Res. Mol. Brain Res. 82, 74–83.
4 Decher, N., Maier, M., Dittrich, W., Gassenhuber, J., Bruggemann, A., Busch, A. E. and Steinmeyer, K. (2001) Characterization of TASK-4, a novel member of the pH-sensitive, two-pore domain potassium channel family. FEBS Lett. 492, 84–89.
5 Duprat, F., Lesage, F., Fink, M., Reyes, R., Heurteaux, C. and Lazdunski, M. (1997) TASK, a human background K^+ channel to sense external pH variations near physiological pH. EMBO J. 16, 5464–5471.
6 Girard, C., Duprat, F., Terrenoire, C., Tinel, N., Fosset, M., Romey, G., Lazdunski, M. and Lesage, F. (2001) Genomic and functional characteristics of novel human pancreatic 2P domain K^+ channels. Biochem. Biophys. Res. Commun. 282, 249–256.
7 Kim, D. and Gnatenco, C. (2001) TASK-5, a new member of the tandem-pore K^+ channel family. Biochem. Biophys. Res. Commun. 284, 923–930.
8 Kim, Y., Bang, H. and Kim, D. (1999) TBAK-1 and TASK-1, two-pore K^+ channel subunits: kinetic properties and expression in rat heart. Am. J. Physiol. 277, H1669–H1678.
9 Kim, Y., Bang, H. and Kim, D. (2000) TASK-3, a new member of the tandem pore K^+ channel family. J. Biol. Chem. 275, 9340–9347.
10 Leonoudakis, D., Gray, A. T., Winegar, B. D., Kindler, C. H., Harada, M., Taylor, D. M., Chavez, R. A., Forsayeth, J. R. and Yost, C. S. (1998) An open rectifier potassium channel with two pore domains in tandem cloned from rat cerebellum. J. Neurosci. 18, 868–877.
11 Rajan, S., Wischmeyer, E., Xin Liu, G., Preisig-Müller, R., Daut, J., Karschin, A. and Derst, C. (2000) TASK-3, a novel tandem pore domain acid-sensitive K^+ channel. An extracellular histidin as pH sensor. J. Biol. Chem. 275, 16650–16657.
12 Reyes, R., Duprat, F., Lesage, F., Fink, M., Salinas, M., Farman, N. and Lazdunski, M. (1998) Cloning and expression of a novel pH-sensitive two pore domain K^+ channel from human kidney. J. Biol. Chem. 273, 30863–30869.
13 Karschin, C., Wischmeyer, E., Preisig-Müller, R., Rajan, S., Derst, C., Grzeschik K-H., Daut, J. and Karschin, A. (2001) Expression pattern in brain of TASK-1, TASK-3, and a tandem pore domain K^+ channel subunit, TASK-5, associated with the central auditory nervous system. Mol. Cell. Neurosci. 18, 632–648.

14 Meadows, H. J. and Randall, A. D. (2001) Functional characterisation of human TASK-3, an acid-sensitive two-pore domain potassium channel. Neuropharmacology 40, 551–559.
15 Lauritzen, I., Zanzouri, M., Honoré, E., Duprat, F., Ehrengruber, M. U., Lazdunski, M. and Patel, A. J. (2003) K^+-dependent cerebellar granule neuron apoptosis. J. Biol. Chem. 278, 32068–32076.
16 Liu, C., Cotton, J. F., Schuyler, J. A., Fahlman, C. S., Au, J. D., Bickler, P. E., Yost, C. S. (2005) Protective effects of TASK-3 (KCNK9) and related 2P K channels during cellular stress. Brain Res. 1031, 164–173.
17 Mu, D., Chen, L., Zhang, X., See L-H., Koch, C. M., Yen, C., Tong, J. J., Spiegel, L., Nguyen, K. C. Q., Servoss, A., Peng, Y., Pei, L., Marks, J. R., Lowe, S., Hoey, T., Jan, L. Y., McCombie, W. R., Wigler, M. H. and Powers, S. (2003) Genomic amplification and oncogenic properties of the KCNK9 potassium channel gene. Cancer Cell 3, 297–302.
18 Pei, L., Wiser, O., Slavin, A., Mu, D., Powers S,. Jan, L. Y. and Hoey, T. (2003) Oncogenic potential of TASK3 (Kcnk9) depends on K^+ channel function. Proc. Natl. Acad. Sci. USA 100, 7803–7807.
19 Cooper, B. Y., Johnson, R. D. and Rau, K. K. (2004) Characterization and function of TWIK-related acid sensing K^+ channels in a rat nociceptive cell. Neuroscience 129, 209–224.
20 Kovács, I., Pocsai, K., Czifra, G., Sarkadi, L., Szűcs, G., Nemes, Z. and Rusznák, Z. (2005) TASK-3 immunoreactivity shows differential distribution in the human gastrointestinal tract. Virchows Arch. 446, 402–410.
21 Lin, W., Burks, C. A., Hansen, D. R., Kinnamon, S. C. and Gilbertson, T. A. (2004) Taste receptor cells express pH-sensitive leak K^+ channels. J. Neurophysiol. 92, 2909–2919.
22 Rusznák, Z., Pocsai, K., Kovács, I., Pór, Á., Pál, B., Bíró, T. and Szűcs, G. (2004) Differential distribution of TASK-1, TASK-2 and TASK-3 immunoreactivities in the rat and human cerebellum. Cell. Mol. Life Sci. 61, 1532–1542.
23 Yamamoto, Y., Kummer, W., Atoji, Y. and Suzuki, Y. (2002) TASK-1, TASK-2, TASK-3 and TRAAK immunoreactivities in the rat carotid body. Brain Res. 950, 304–307.
24 Yamamoto, Y. and Taniguchi, K. (2003) Heterogeneous expression of TASK-3 and TRAAK in rat paraganglionic cells. Histochem. Cell Biol. 120, 335–339.
25 Carlson, J. A., Slominski, A., Linette, G. P., Mihm, M. C. Jr. and Ross, J. S. (2003) Biomarkers in melanoma: predisposition, screening and diagnosis. Expert Rev. Mol. Diagn. 3, 163–184..
26 Tímár, J., Raso, E., Honn, K. V. and Hagmann, W. (1999) 12-lipoxygenase expression in human melanoma cell lines. Adv. Exp. Med. Biol. 469, 617–622.
27 Diaz-Guerra, M. J., Velasco, M., Martin-Sanz, P. and Bosca, L. (1996) Evidence for common mechanisms in the transcriptional control of type II nitric oxide synthase in isolated hepatocytes. Requirement of NF-kappaB activation after stimulation with bacterial cell wall products and phorbol esters. J. Biol. Chem. 22, 30114–30120.
28 Roberts, T. G., Sturm, N. R., Yee, B. K., Yu, M. C., Hartshorne, T., Agabian, N. and Campbell, D. A. (1998) Three small nucleolar RNAs identified from the spliced leader-associated RNA locus in kinetoplastid protozoans. Mol. Cell. Biol. 18, 4409–4417.
29 Czirják, G. and Enyedi, P. (2003) TASK-3 dominates the background potassium conductance in rat adrenal glomerulosa cells. Mol. Endocrinol. 16, 621–629.
30 Callahan, R., Labunskiy, D. A., Logvinova, A., Abdallah, M., Liu, C., Cotton, J. F. and Yost, C. S. (2004) Immunolocalization of TASK-3 (KCNK9) to a subset of cortical neurons in the rat CNS. Biochem. Biophys. Res. Commun. 319, 525–530.
31 Hartness, M. E., Lewis, A., Searle, G. J., O'Kelly, I., Peers, C. and Kemp, P. J. (2001) Combined antisense and pharmacological approaches implicate hTASK as an airway O_2 sensing K^+ channel. J. Biol. Chem. 276, 26499–26508.
32 Washburn, C. P., Sirois, J. E., Talley, E. M., Guyenet, P. G. and Bayliss, D. A. (2002) Serotonergic raphe neurons express TASK channel transcripts and a TASK-like pH- and halothane-sensitive K^+ conductance. J. Neurosci. 22, 1256–1265.
33 Washburn, C. P., Bayliss, D. A. and Guyenet, P. G. (2003) Cardiorespiratory neurons of the rat ventrolateral medulla contain TASK-1 and TASK-3 channel mRNA. Respir. Physiol. Neurobiol. 138, 19–35.
34 Williams, B. A. and Buckler, K. J. (2004) Biophysical properties and metabolic regulation of a TASK-like potassium channel in rat carotid body type 1 cells Am. J. Physiol. 286, L221–L230.
35 Aller, M. I., Veale, E. L., Linden A-M., Sandu, C., Schwaninger, M., Evans, L. J., Korpi, E. R., Mathie, A., Wisden, W. and Brickley, S. G. (2005) Modifying the subunit composition of TASK channels alters the modulation of a leak conductance in cerebellar granule neurons. J. Neurosci. 25, 11455–11467.
36 Berg, A. P., Talley, E. M., Manger, J. P. and Bayliss, D. A. (2004) Motoneurons express heteromeric TWIK-related acid-sensitive K^+ (TASK) channels containing TASK-1 (KCNK3) and TASK-3 (KCNK9) subunits. J. Neurosci. 24, 6693–6702.
37 Chemin, J., Girard, C., Duprat, F., Lesage, F., Romey, G. and Lazdunski, M. (2003) Mechanisms underlying excitatory effects of group I metabotropic glutamate receptors via inhibition of 2P domain K^+ channels. EMBO J. 22, 5403–5411.
38 Han, J., Truell, J., Gnatenco, C. and Kim, D. (2002) Characterization of four types of background potassium channels in rat cerebellar granule neurons. J. Physiol. 542, 431–444.
39 Hopwood, S. E. and Trapp, S. (2005) TASK-like K^+ channels mediate effects of 5-HT and extracellular pH in rat dorsal vagal neurones *in vitro*. J. Physiol. 568, 145–154.
40 Kang, D., Han, J., Talley, E. M., Bayliss, D. A. and Kim, D. (2003) Functional expression of TASK-1/TASK-3 heteromers in cerebellar granule cells. J. Physiol. 554, 64–77.
41 Meuth, S. G., Budde, T., Kanyshkova, T., Broicher, T., Munsch, T. and Pape H-C. (2003) Contribution of TWIK-related acid-sensitive K^+ channel 1 (TASK1) and TASK3 channels to the control of activity modes in thalamocortical neurons. J. Neurosci. 23, 6460–6469.
42 Han, J., Gnatenco, C., Sladek, C. D. and Kim, D. (2003) Background and tandem-pore potassium channels in magnocellular neurosecretory cells of the rat supraoptic nucleus. J. Physiol. 546,625–639.
43 Patel, A. J. and Lazdunski, M. (2004) The 2P-domain K^+ channels: role in apoptosis and tumorigenesis. Pflügers Arch. 448, 261–273.
44 Buckler, K. J., Williams, B. A. and Honore, E. (2000) An oxygen-, acid- and anaesthetic-sensitive TASK-like background potassium channel in rat arterial chemoreceptor cells. J. Physiol. 525, 135–142.
45 Talley, E. M. and Bayliss, D. A. (2002) Modulation of TASK-1 (Kcnk3) and TASK-3 (Kcnk9) potassium channels. J. Biol. Chem. 277, 17733–17742.
46 Kim, C. J., Cho, Y. G., Jeong, S. W., Kim, Y. S., Kim, S. Y., Nam, S. W., Lee, S. H., Yoo, N. J., Lee, J. Y. and Park, W. S. (2004) Altered expression of KCNK9 in colorectal cancers. APMIS 112, 588–594.
47 Czirják, G. and Enyedi, P. (2002) Formation of functional heterodimers between the TASK-1 and TASK-3 two-pore domain potassium channel subunits. J. Biol. Chem. 277, 5426–5432.
48 Rajan, S., Preisig-Müller, R., Wischmeyer, E., Nehring, R., Hanley, P. J., Renigunta, V., Musset, B., Schlichthörl, G., Derst, C., Karschin, A. and Daut, J. (2002) Interaction with 14-3-3 proteins promotes functional expression of the potassium channels TASK-1 and TASK-3. J. Physiol. 545, 13–26.